Supporting Information for

Highly dispersed ultrafine Ni particles embedded into MOF-74 arrays by partial carbonization for highly efficient hydrogen evolution

Jing-Bo Tan, Jing-Qi Wu, Jia-Wei Zhao, Ling-Jie Xie, and Gao-Ren Li*

MOE Key Laboratory of Bioinorganic and Synthetic Chemistry, School of Chemistry, Sun Yat-Sen University, Guangzhou 510275, China.

Experimental

Preparation of bulk Ni-MOF-74 electrodes. Typically, 8.0 mg Ni-MOF-74, 10 μl 5% nafion and 500 μl ethanol was sonicated at least 30 min to form the ink. And then the ink was dropped into 1 × 1 cm NF and dried by hot air. All Ni foam electrode substrates were etched in 3.0 M HCl solution for 30 min to remove the native nickel oxide on the surface and was washed by DI water several times prior to pasting.

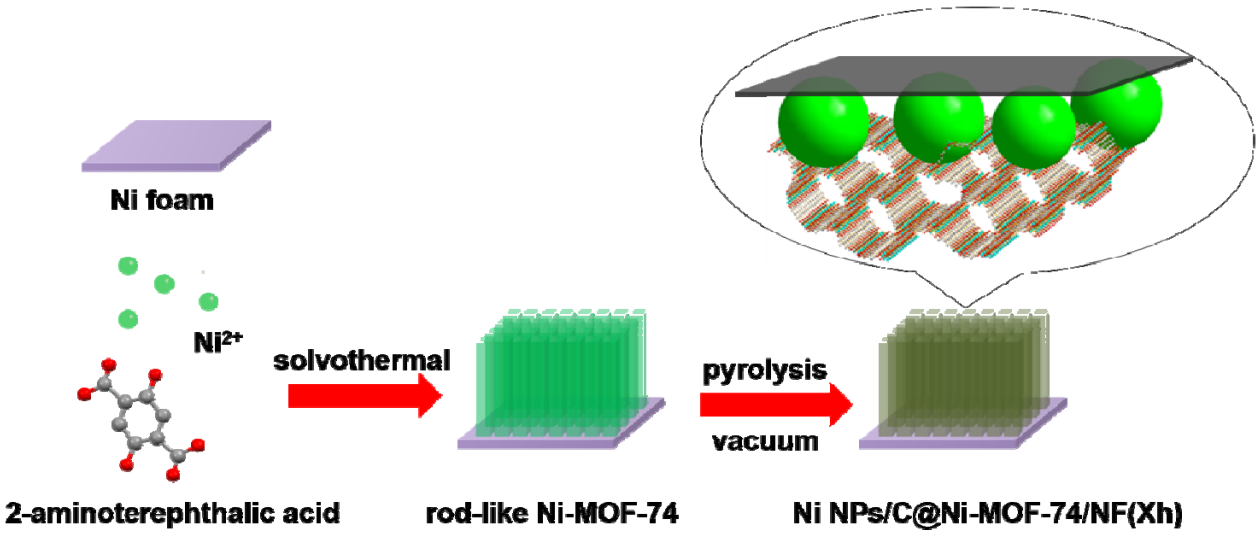

Scheme S1. The synthesis scheme of Ni NPs/C@Ni-MOF-74/NF.

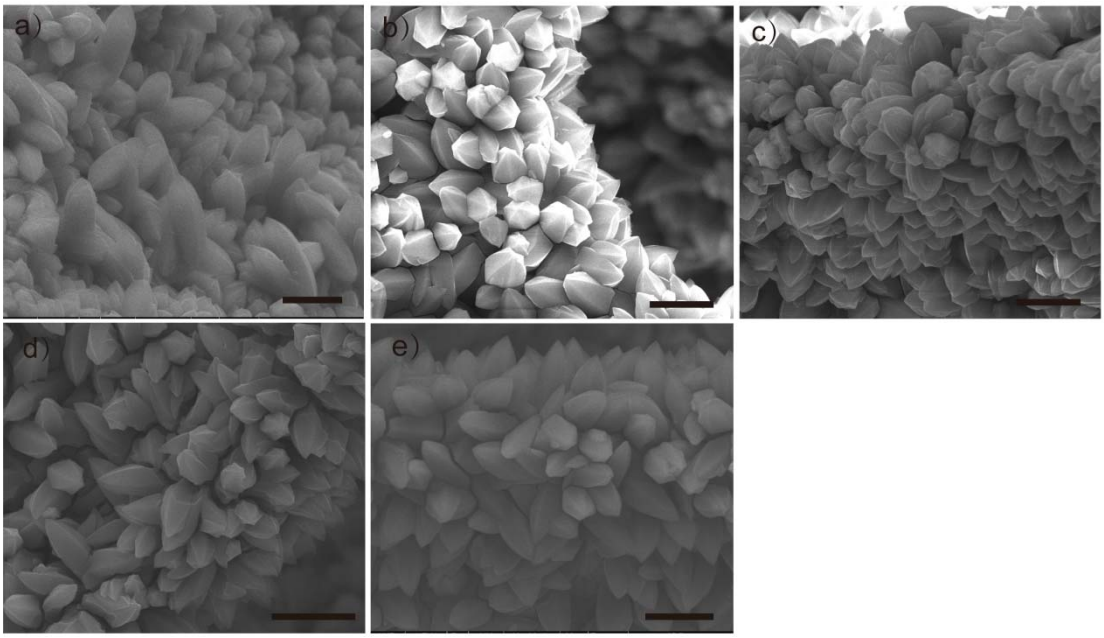

Fig. S1 a) SEM image of Ni-MOF-74/NF; SEM images of b) Ni NPs/C@Ni-MOF-74(6 h), c) Ni NPs/C@Ni-MOF-74(12 h), d) Ni NPs/C@Ni-MOF-74(18 h), and e) Ni NPs/C@Ni-MOF-74(24 h) (black scale bar is 10 μm).

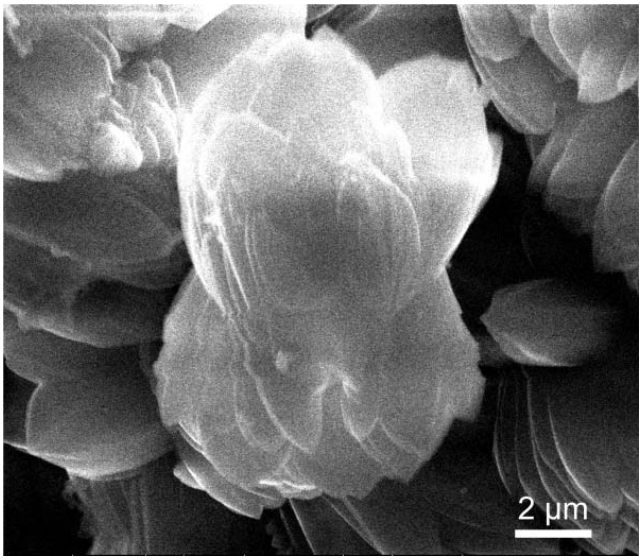

Fig. S2 SEM image of Ni-MOF-74.

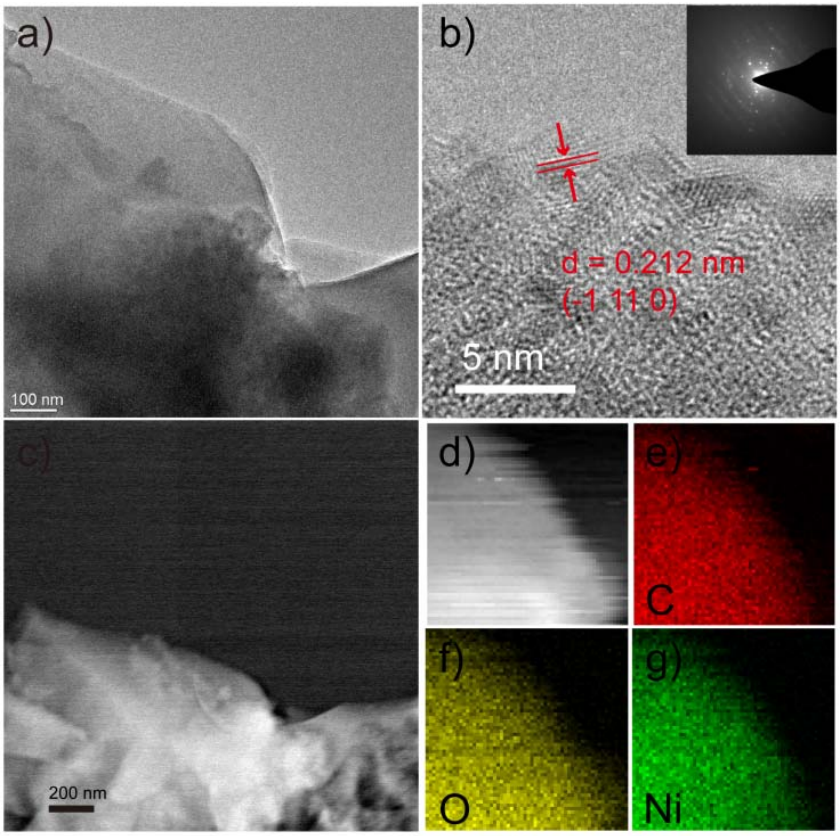

Fig. S3 a) TEM image; b) HRTEM image with electron diffraction (inset); c) STEM image; d) HADDF-STEM image; d-g) elemental mappings of Ni-MOF-74.

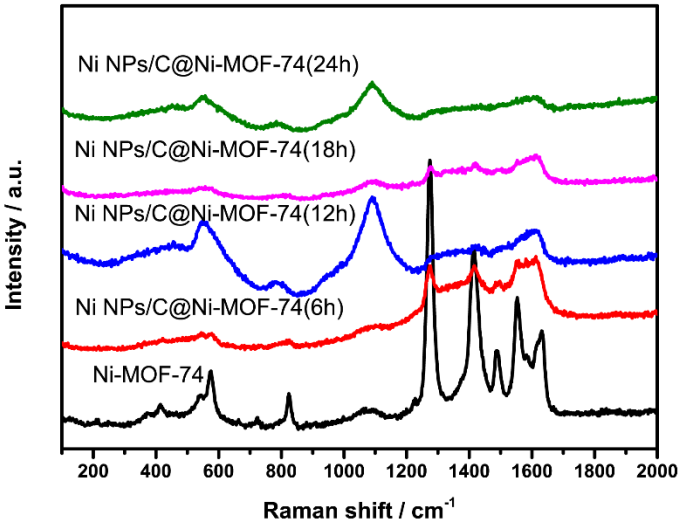

Fig. S4 Raman spectra of Ni-MOF-74/NF, Ni NPs/C@Ni-MOF-74(6 h), Ni NPs/C@Ni-MOF-74(12 h), Ni NPs/C@ Ni-MOF-74(18 h), and Ni NPs/C@Ni-MOF-74(24 h).

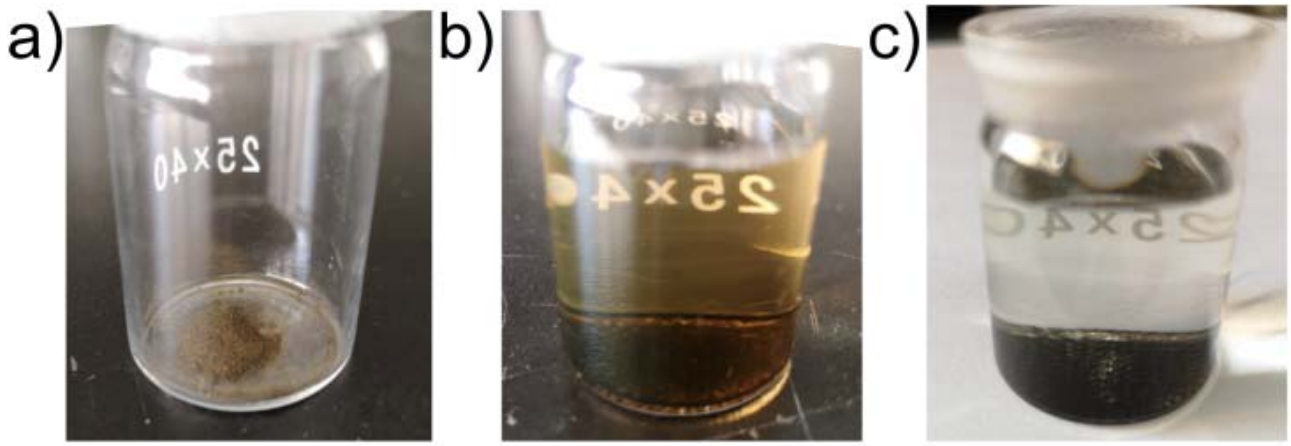

Fig. S5 Optical images of a) initial Ni NPs/C@Ni-MOF-74(18 h), b) Ni NPs/C@Ni-MOF-74(18 h) treated with 0.1M HCl, and c) Ni NPs/C@Ni-MOF-74(18 h) rinsed with 0.1M HCl.

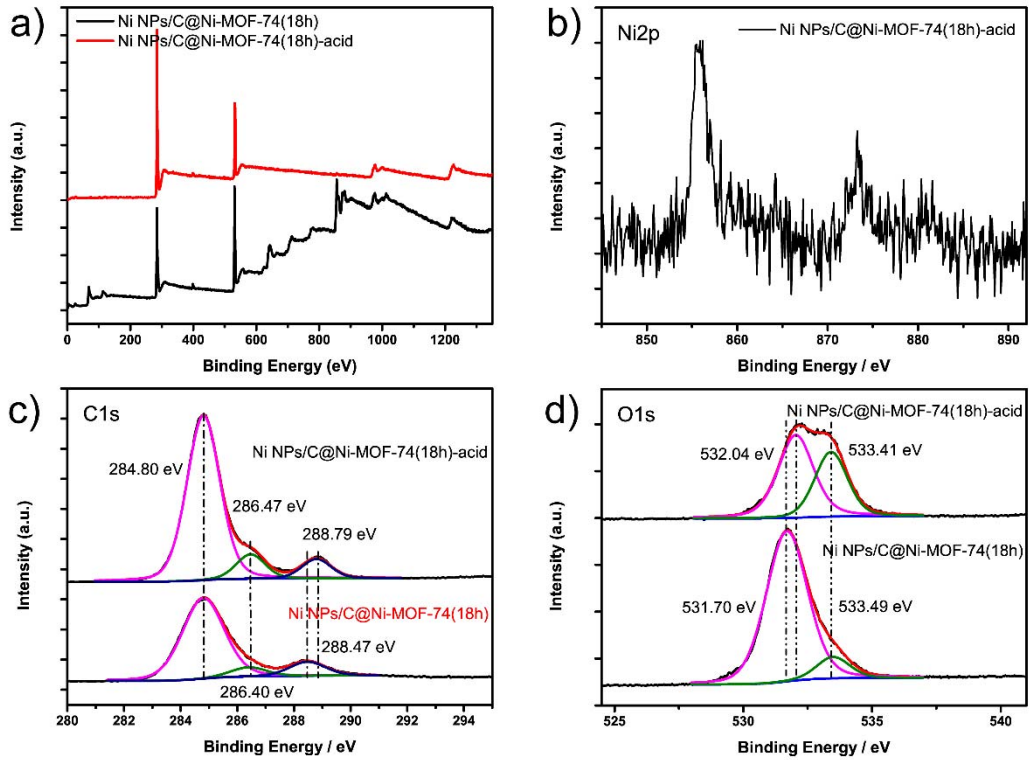

Fig. S6 a) XPS survey spectra of Ni NPs/C@Ni-MOF-74(18 h) before and after HCl treatment; b) XPS spectrum of Ni 2p of Ni NPs/C@Ni-MOF-74(18 h) after HCl treatment; c) XPS spectra of C1s and d) O 1s of Ni NPs/C@Ni-MOF-74(18 h) before and after HCl treatment.

In detail, the residue is carbon since the Ni NPs/C@Ni-MOF-74(18 h) frameworks are all collapsed after

acid treatment. With the comparison of both full XPS spectra, a big change occurs after acid treatment. In addition, the weak signals of Ni 2p core peaks are observed as shown in Figure S6b, implying that only few Ni^{2+} ions are absorbed by the carbon residue. In addition, XPS spectra of C 1s and O 1s of Ni NPs/C@Ni-MOF-74(18h) after acid treatment also confirms the residue is carbon because they are different from those of the ligand (2-aminoterephthalic acid) inside the frameworks.

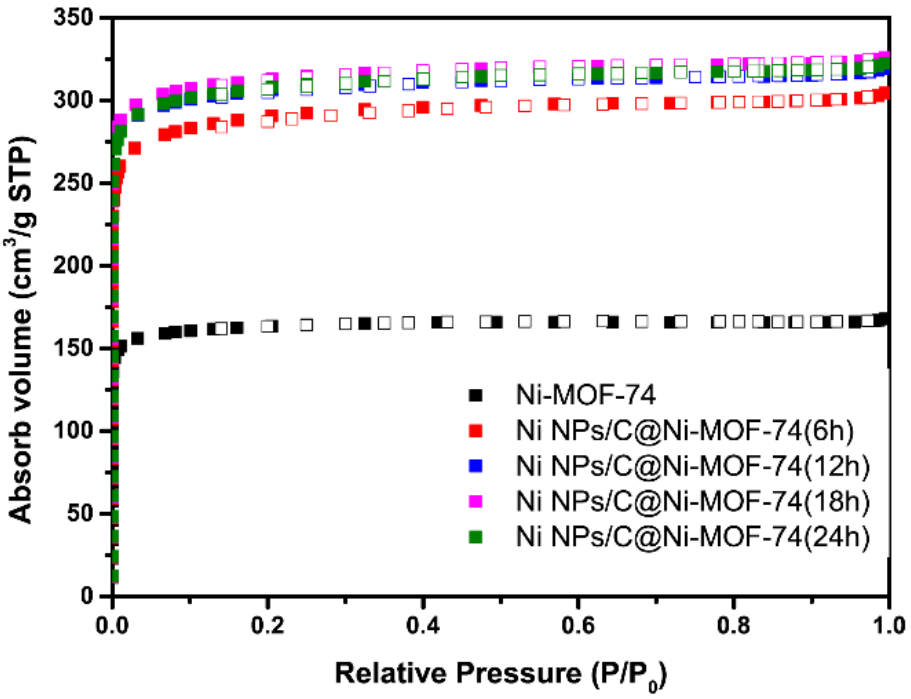

Fig. S7 N_2 adsorption-desorption isotherms of Ni-MOF-74/NF, Ni NPs/C@Ni-MOF-74(6 h), Ni NPs/C@Ni-MOF-74(12 h), Ni NPs/C@Ni-MOF-74(18 h), and Ni NPs/C@Ni-MOF-74(24 h) at 77K.

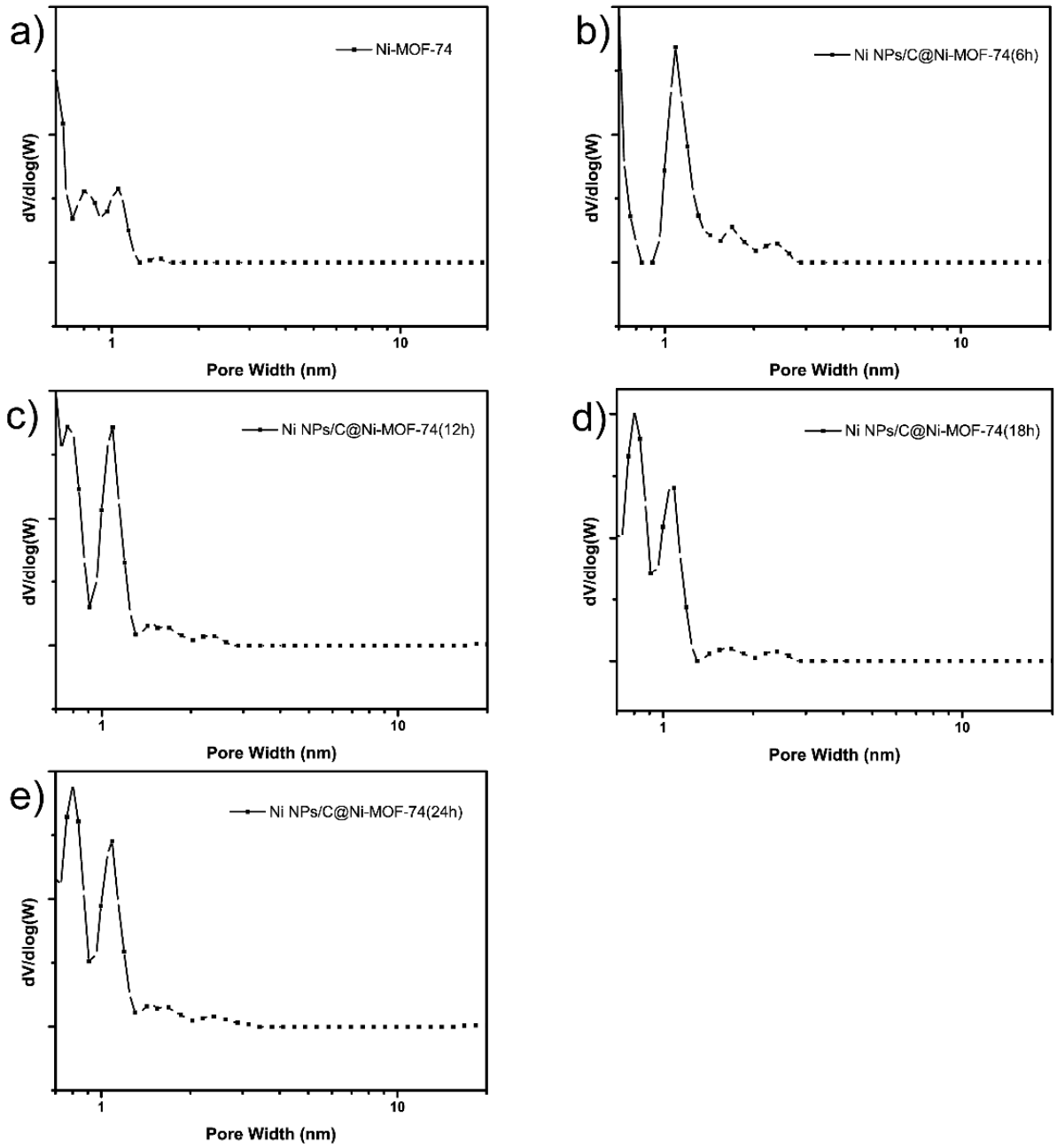

Fig. S8 Pore size distribution plots of Ni-MOF-74/NF, Ni NPs/C@Ni-MOF-74(6 h), Ni NPs/C@Ni-MOF-74(12 h), Ni NPs/C@ Ni-MOF-74(18 h), and Ni NPs/C@Ni-MOF-74(24 h).

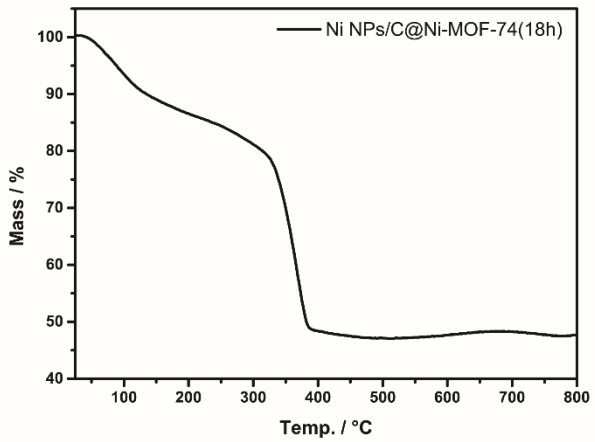

Fig. S9 TGA curve of Ni NPs/C@Ni-MOF-74(18 h) under air atmosphere up to 800 ℃.

As we know, the formula of Ni-MOF-74 was $Ni_2(C_8H_6O_8)$, M_w = 347.51. The decompose chemical equation of the generated Ni NPs/C@Ni-MOF-74 is assumed that:

$$Ni_2(C_8H_6O_8) \rightarrow 2Ni + 5C + 2CO_2\uparrow + CO\uparrow + 3H_2O$$

Given that m_{total} = 2.26 mg, $m_{residure}$ = 1.09 mg

$n_{Ni\text{-}MOF\text{-}74} = (m_{total} \times 0.001 - ((58.69 + 60.00) \div 74.69 \times m_{residure} \times 0.001)) / (347.51 - 2 \times (58.69 + 60.00)) = 4.72 \times 10^{-6}$ mol

$n_{Ni} = (m_{residure} \times 0.001 / 74.69) - (2 \times n_{Ni\text{-}MOF\text{-}74}) = 5.21 \times 10^{-6}$ mol

Molar ratio of Ni : Ni-MOF-74 ≈ 1.1 : 1

Mass ratio of Ni particles in Ni NPs/C@Ni-MOF-74(18 h) $\omega = n_{Ni} \times 58.69 \div (m_{total} \times 0.001)$ = 13.55 %

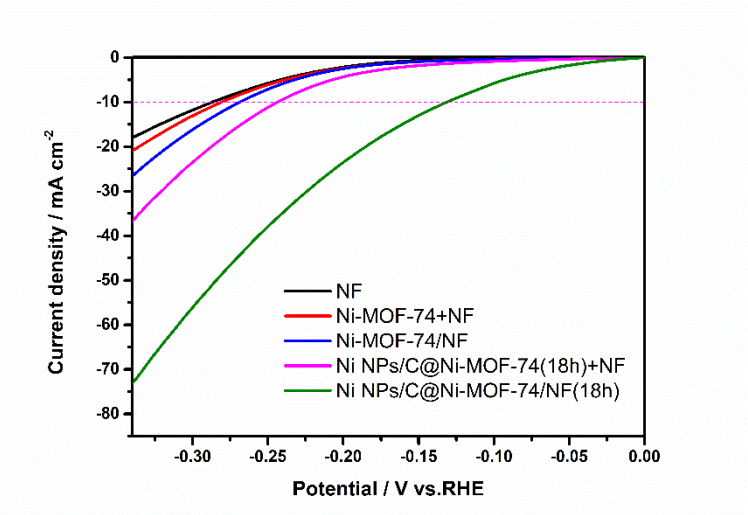

Fig. S10 LSVs of Ni NPs/C@Ni-MOF-74/NF(18 h), Ni-MOF-74/NF and their counterparts.

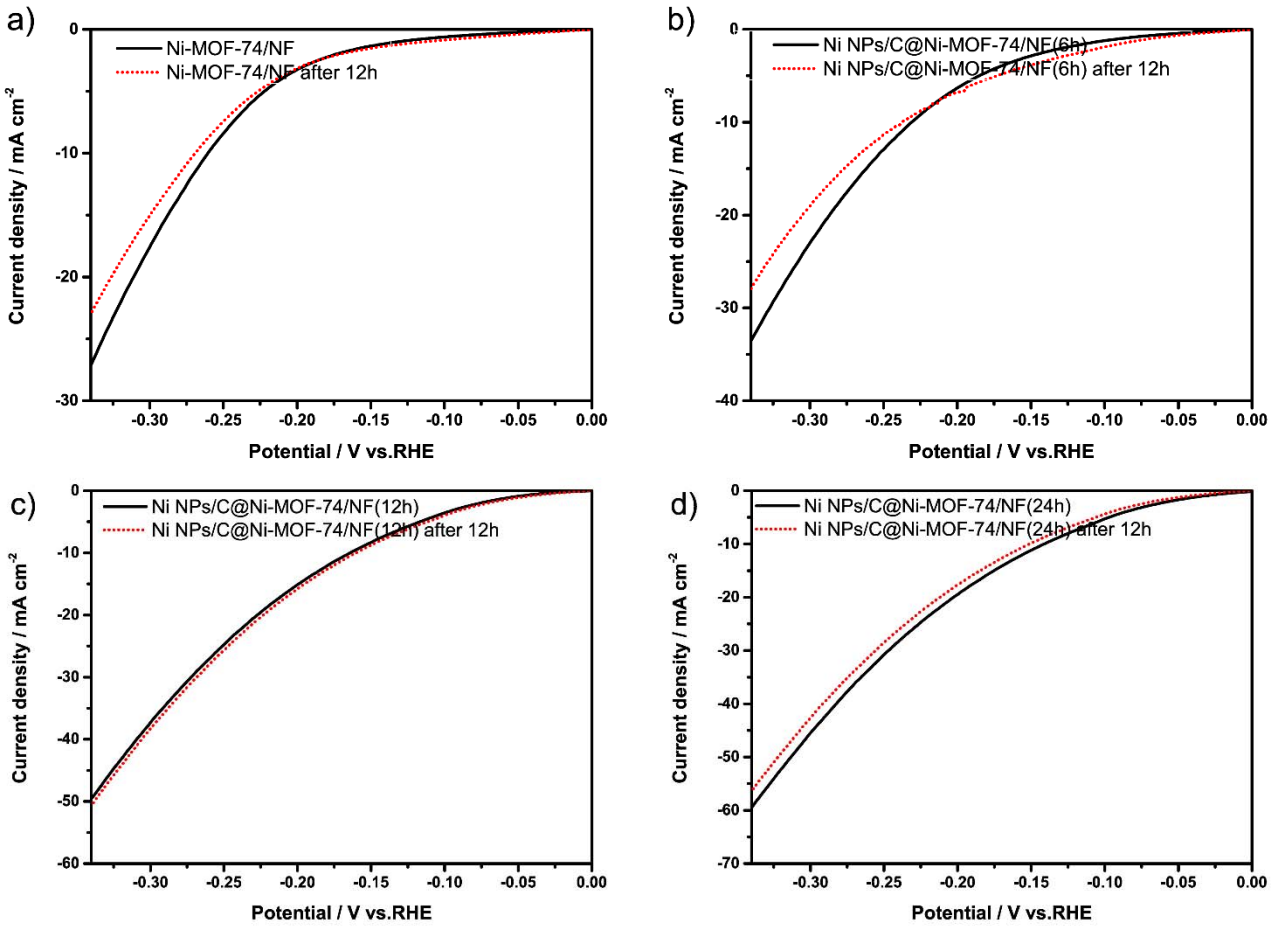

Fig. S11 LSVs of all as-prepared catalysts before and after 12 h electrolysis.

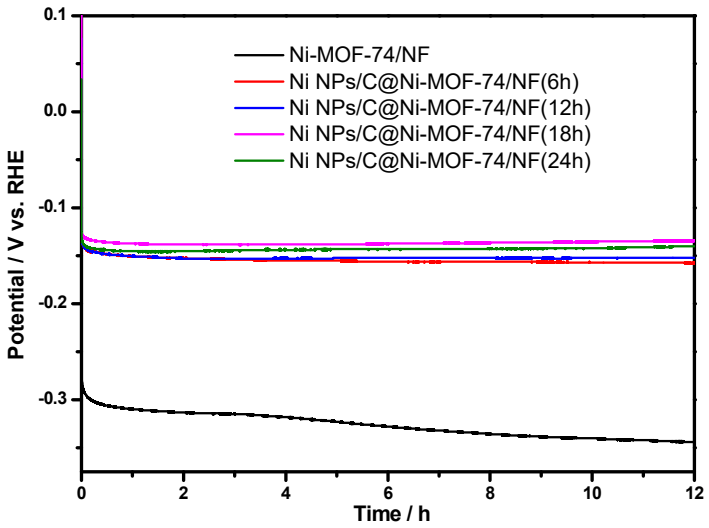

Fig. S12 Chronopotentiometric curves of various catalysts at current density of 10 mA cm^{-2}.

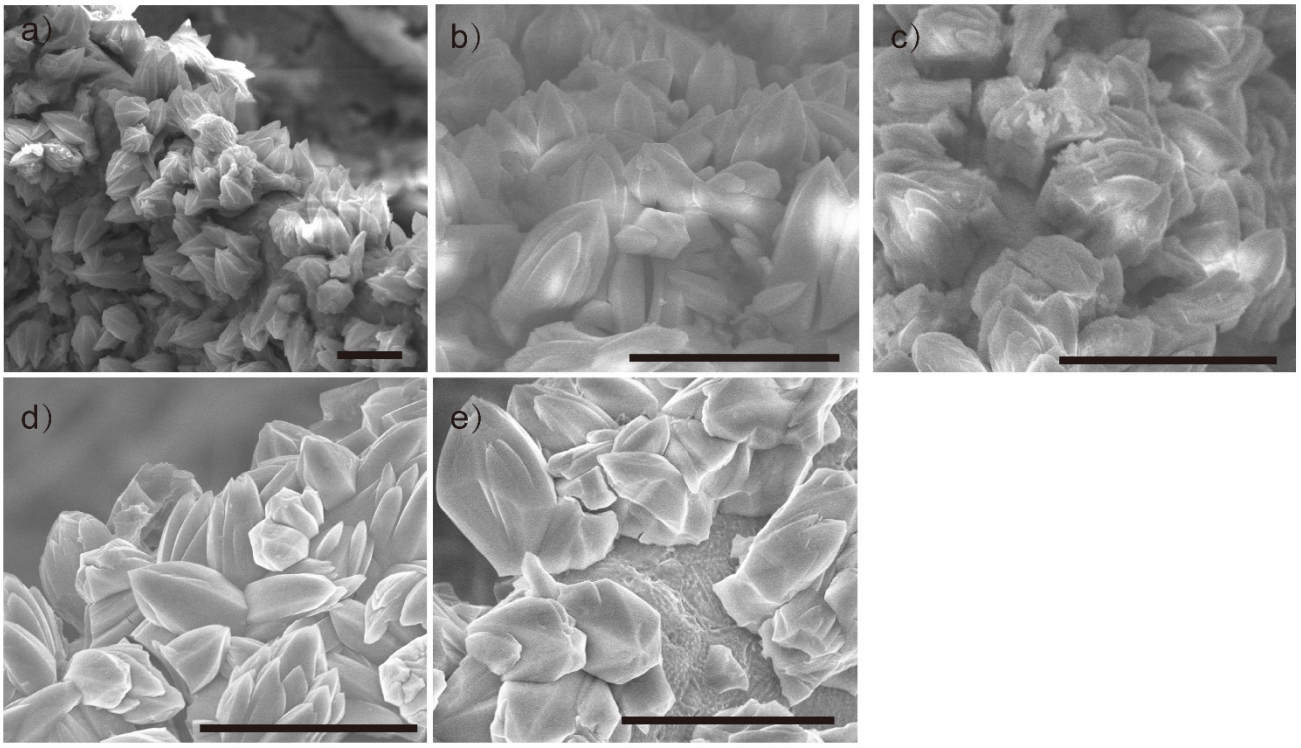

Fig. S13 SEM images of a) Ni-MOF-74/NF, b) Ni NPs/C@Ni-MOF-74(6 h), c) Ni NPs/C@Ni- MOF-74(12 h), d) Ni NPs/C@Ni-MOF-74(18 h), and e) Ni NPs/C@Ni-MOF-74(24 h) after durability tests (black scale bar is 10 μm).

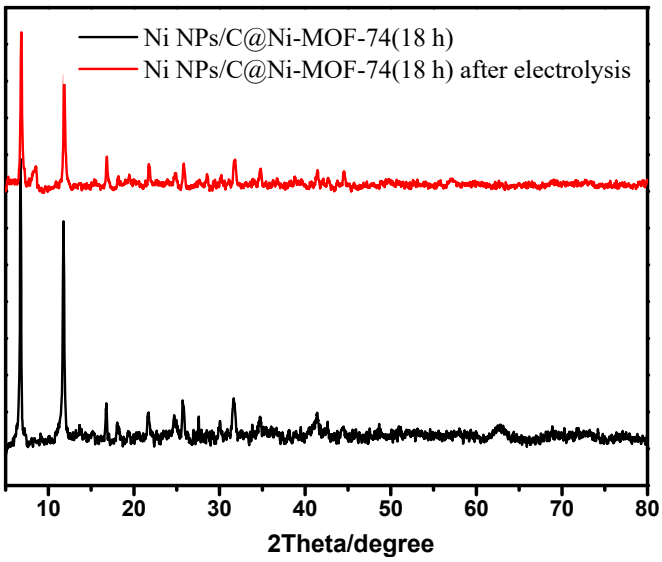

Fig. S14 PXRD patterns of Ni NPs/C@Ni-MOF-74(18 h) before and after durability test.

Table S1. Comparisons of HER activities over MOF-based electrocatalysts in alkaline solution.

HER catalyst	Electrolyte	Overpotential [a] / mV	Tafel slope / mV dec^{-1}	Stability tests [b]	Ref.
Ni-MOF-74 arrays /NF	1.0 M KOH	269	133	12 h gradually decay	This work
Ni NPs/C@Ni-MOF-74/NF(6 h)	1.0 M KOH	183	117	12 h slightly decay	This work
Ni NPs/C@Ni-MOF-74/NF(12 h)	1.0 M KOH	165	108	12 h	This work
Ni NPs/C@Ni-MOF-74/NF(18 h)	1.0 M KOH	131	104	48 h	This work
Ni NPs/C@Ni-MOF-74/NF(24 h)	1.0 M KOH	143	106	12 h	This work
NiFe-MOF array/NF	0.1 M KOH	134	N/A	2000 s	1
NFN-MOF/NF	1.0 M KOH	87	35	30 h 8.0% decay	2
MFN-MOFs/NF	1.0 M KOH	79	30	N/A	3
Ni_2P Ps-3	1.0 M KOH	158	73	20 h	4
Co_3S_4/EC-MOF	1.0 M KOH	84	82	24 h	5
Co-NC/CNT-800	1.0 M KOH	203	125	1000 cycles and 30000 s	6
Co/Co_9S_8@ SNGS-1000	0.1 M KOH	350 mV at 20 mA cm^{-2}	96	1000 cycles	7
Ni@graphene	1.0 M KOH	240	120	10 h	8
NCF-MOF	0.1 M KOH	110	114	20000 s	9
Fe-Ni@NC-CNTs	1.0 M KOH	202	114	40000 s	10
HUST-200	acidic aqueous medium	131	51	9 h	11
AB&CTGU9(3: 4)	0.5 M H_2SO_4	128	87	21 h	12
UU-100(Co)	pH = 4 0.2 M acetate buffer	N/A	250	5 h	13
Ni-NiO/C HPPAs	1.0 M KOH	49	74	30 h 3.7% decay	14
NiFeSe@NiSe|O@CC	1.0 M KOH	40	49	50 h 3.5%decay	15
NiCoFeP/C	1.0 M KOH	149	108	20 h	16
Ni-ZIF/Ni-B@NF	1.0 M KOH	67	108	64 h	17
Ni@NC (NH_3-plasma MOF-74-Ni)	1.0 M KOH	61	89	18 h slight decay	18
$Ni_3(Ni_3$·HAHATN$)_2$	0.1 M KOH	115	45	10 h 27% decay and 1000 cycles	19

a) Overpotential is measured at 10 mA cm^{-2}; b) the duration of the chronoamperometric (or chronopotentiometric) results and the number of CV cycles are summarized in this table (the current density decrease after CV cycles and chronoamperometric curve decrease denote "decay").

Table S2. EIS results of Ni-MOF-74/NF, Ni NPs/C@Ni-MOF-74(6 h), Ni NPs/C@Ni-MOF-74(12 h), Ni NPs/C@Ni-MOF-74 (18 h), and Ni NPs/C@Ni-MOF-74(24 h).

Electrode	R_s (Ω)	R_{ct} (Ω)
Ni-MOF-74/NF	2.67	6.98
Ni NPs/C@Ni-MOF-74/NF(6 h)	2.47	5.97
Ni NPs/C@Ni-MOF-74/NF(12 h)	2.40	4.87
Ni NPs/C@Ni-MOF-74/NF(18 h)	2.05	3.69
Ni NPs/C@Ni-MOF-74/NF(24 h)	1.84	4.30

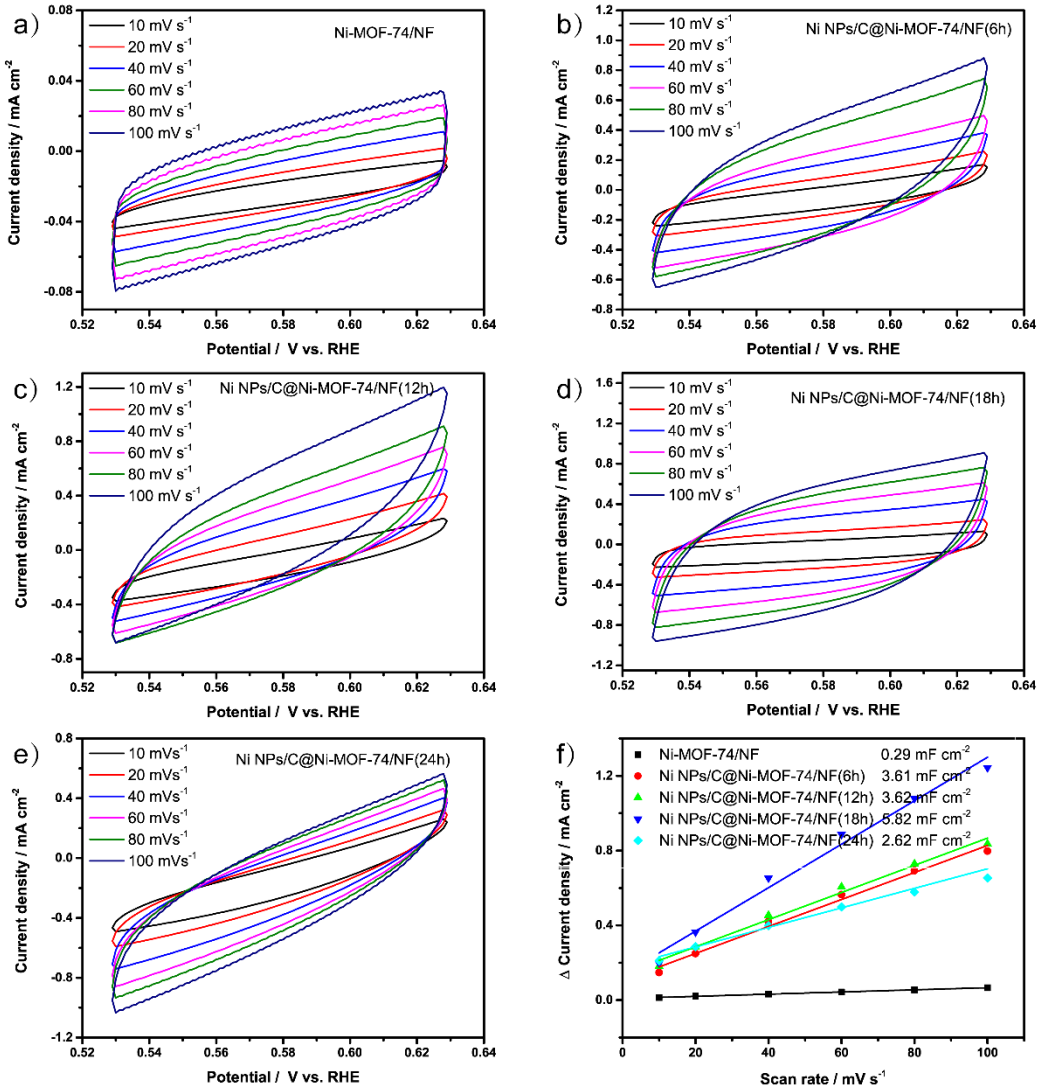

Fig. 15 a-e) CVs of all samples with different treatment time in 1.0 M KOH solution at varying scan rates, f) The plots of the capacitive current density Δ*j* as a function of scan rates.

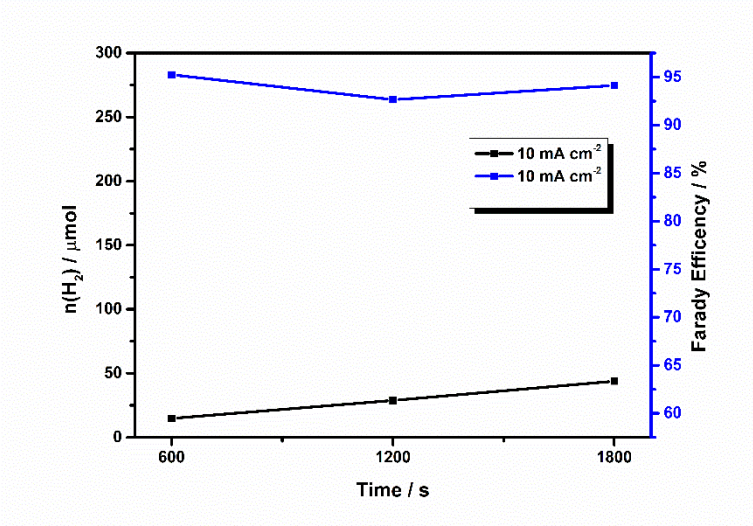

Fig. S16 The experimental H_2 product amount of Ni NPs/C@Ni-MOF-74/NF(18 h) at 10 mA cm^{-2} and the corresponding Faraday efficiency.

The Faraday efficiency of Ni NPs/C@Ni-MOF-74/NF(18 h) was measured at the current density of 10 mA cm^{-2}. The operation measurement of the Faraday Efficiency shows as follows: A piece of Ni NPs/C@Ni-MOF-74/NF(18 h) (surface area = 0.5 cm^2) was immersed in the electrolyte as the working electrode. The head space volume of the electrolytic cell and the volume of solution were measured to be 35.0 and 21.0 mL, respectively. Before measurement, the cell was purged by Ar gas for about 30 min to eliminate the air background. The hydrogen concentrations were measured using gas chromatography (GC, Agilent 7820A) equipped with Molecular sieve 5 Å capillary column and thermal conductivity detector. The Faraday Efficiency at 10 mA cm^{-2} with time increasing was kept around 93%.

References

1. J. Duan, S. Chen and C. Zhao, *Nat. Commun.*, 2017, **8**, 15341.
2. D. S. Raja, X. F. Chuah and S. Y. Lu, *Adv. Energy Mater.*, 2018, **8**, 1801065.
3. D. Senthil Raja, H.-W. Lin and S.-Y. Lu, *Nano Energy*, 2019, **57**, 1-13.
4. L. Yan, P. Dai, Y. Wang, X. Gu, L. Li, L. Cao and X. Zhao, *ACS Appl. Mater. Interfaces*, 2017, **9**, 11642-11650.
5. T. Liu, P. Li, N. Yao, T. Kong, G. Cheng, S. Chen and W. Luo, *Adv. Mater.*, 2019, **31**, 1806672.
6. F. L. Yang, P. P. Zhao, X. Hua, W. Luo, G. Z. Cheng, W. Xing and S. L. Chen, *J. Mater. Chem. A*, 2016, **4**, 16057.
7. X. Zhang, S. W. Liu, Y. P. Zang, R. R. Liu, G. Q. Liu, G. Z. Wang, Y. X. Zhang, H. M. Zhang and H. J. Zhao,

Nano Energy, 2016, **30**, 93-102.

8. L. H. Ai, T. Tian and J. Jiang, *ACS Sustainable Chem. Eng.*, 2017, **5**, 4771-4777.
9. W. Ahn, M. G. Park, D. U. Lee, M. H. Seo, G. P. Jiang, Z. P. Cano, F. M. Hassan and Z. W. Chen, *Adv. Funct. Mater.*, 2018, **28**, 1802129.
10. X. Zhao, P. Pachfule, S. Li, J. R. J. Simke, J. Schmidt and A. Thomas, *Angew. Chem., Int. Ed.*, 2018, **57**, 8921-8926.
11. L. Zhang, S. Li, C. J. Gomez-Garcia, H. Ma, C. Zhang, H. Pang and B. Li, *ACS Appl. Mater. Interfaces*, 2018, **10**, 31498-31504.
12. W. Zhou, Y. P. Wu, X. Wang, J. W. Tian, D. D. Huang, J. Zhao, Y. Q. Lan and D. S. Li, *CrystEngComm*, 2018, **20**, 4804-4809.
13. S. Roy, Z. Huang, A. Bhunia, A. Castner, A. K. Gupta, X. Zou and S. Ott, *J. Am. Chem. Soc.*, 2019, **141**, 15942-15950.
14. W. Zhou, X. F. Lu, J. J. Chen, T. Zhou, P. Q. Liao, M. Wu and G. R. Li, *ACS Appl. Mater. Interfaces*, 2018, **10**, 38906-38914.
15. C. Yilmaz, C. F. Tan, Y. F. Lim and C. W. Ho, *Adv. Energy Mater.*, 2019, **9**, 1802983.
16. X. Wei, Y. Zhang, H. He, L. Peng, S. Xiao, S. Yao and P. Xiao, *Chem. Commun.*, 2019, **55**, 10896-10899.
17. H. Xu, B. Fei, G. Cai, Y. Ha, J. Liu, H. Jia, J. Zhang, M. Liu and R. Wu, *Adv. Energy Mater.*, 2020, **10**, 1902714.
18. Y. Guo, X. Gao, C. Zhang, Y. Wu, X. Chang, T. Wang, X. Zheng, A. Du, B. Wang, J. Zheng, K. Ostrikov and X. Li, *J. Mater. Chem. A*, 2019, **7**, 8129-8135.
19. H. Huang, Y. Zhao, Y. Bai, F. Li, Y. Zhang and Y. Chen, *Adv. Sci.*, 2020, 2000012.